

## Two-domain contact model of volumetric actuators

Jakub Lengiewicz, Michał Kursa and Paweł Hołobut

*Institute of Fundamental Technological Research, Polish Academy of Sciences, Warsaw, Poland*

Summary: We propose a framework for modeling *volumetric actuators*. Finite element implementation details and numerical examples are presented.

### Volumetric actuators

Volumetric actuators are a specific class of actuators whose output forces are generated by micro-actuators distributed over their volumes and working in parallel. Well-designed volumetric actuators have maximum output forces proportional to the number of micro-actuators in their interior, and so to their volumes. This is unlike the usual actuator designs, e.g., hydraulic and pneumatic cylinders or piezoelectric crystals, whose forces are proportional to their cross-sectional areas, not volumes.

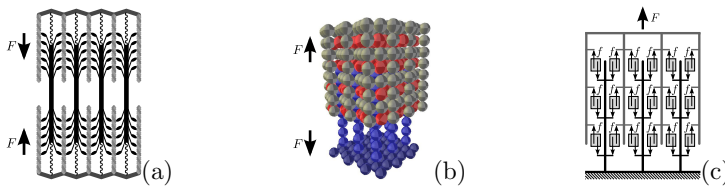


Figure 1: Volumetric actuators: (a) sarcomere, (b) modular-robot, (c) schematic.

A well known example of such systems is the sarcomere [1], which is a fundamental active subunit of animal muscles. In Fig. 1a, a schematic of the sarcomere is presented, with heads of myosin molecules (black) working as micro-actuators, pulling adjacent actin filaments (gray), and producing an overall contracting force. Quite similarly, an artificially designed modular-robotic structure can possibly work as a two-directional actuator [2], see Fig. 1b.

Finally, Fig. 1c shows the general principle of operation of a (linear-motion) volumetric actuator, with two structures pushed/pulled in opposite directions with an overall force  $F$ —a sum of micro-actuations of magnitude  $f$  each. In order to enable finite extensions, each micro-actuator is realized as a contact system that enforces a slip between two constituent parts.

### Two-domain contact model

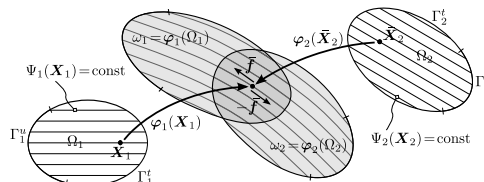


Figure 2: Continuum mechanics model.

In the presented macroscopic actuator model, two inter-penetrating bodies,  $\Omega_1$  and  $\Omega_2$ , move against each other along some permitted directions (isolines  $\Psi_i = \text{const}$ ), see Fig. 2. We assume a possible coupling between the allowed finite deformations and micro-actuation characteristics. Neglecting body forces, the weak form for two interacting actuator parts reads

$$G(\varphi, \delta\varphi) = G_1(\varphi, \delta\varphi_1) + G_2(\varphi, \delta\varphi_2) + G_c(\varphi, \delta\varphi) = 0, \quad (1)$$

where the variations  $\delta\varphi = \{\delta\varphi_1, \delta\varphi_2\}$  vanish on  $\Gamma_i^u$ , the weak forms

$$G_i(\varphi, \delta\varphi_i) = \int_{\Omega_i} \frac{DW_i}{D\mathbf{F}_i} \cdot \nabla \delta\varphi_i dV_i - \int_{\Gamma_i^t} \mathbf{T}_i^* \cdot \delta\varphi_i dS_i, \quad i \in \{1, 2\} \quad (2)$$

are derived from (hyper)elastic potentials  $W_i$  with deformation gradients  $\mathbf{F}_i = \nabla\varphi_i$ ,

$$G_c(\varphi, \delta\varphi) = \int_{\bar{\Omega}_1} \left[ \rho(\Psi_1(\mathbf{X}_1) - \Psi_2(\bar{\mathbf{X}}_2)) \frac{\partial\Psi_2}{\partial\bar{\mathbf{X}}_2} (\nabla\bar{\varphi}_2)^{-1} + \bar{f} \frac{\mathbf{F}_1 \nabla\bar{\Psi}_1}{\|\mathbf{F}_1 \nabla\bar{\Psi}_1\|} \right] \cdot (\delta\varphi_1 - \delta\varphi_2) dV_1 \quad (3)$$

is the *contact part* of the weak form (1), in which  $\bar{\mathbf{X}}_2$  is a point of  $\Omega_2$  such that  $\bar{\varphi}_2 = \varphi_2(\bar{\mathbf{X}}_2)$  coincides with the point  $\varphi_1(\mathbf{X}_1)$  (note here that volumetric contact search is needed),  $\bar{\Omega}_1 = \varphi_1^{-1}(\omega_1 \cap \omega_2)$ , and  $\bar{\Psi}_1$  is so defined that  $\nabla\bar{\Psi}_1$  are parallel to the isolines of  $\Psi_1$ . The first term in (3) is the enforcement of the condition that corresponding isolines of  $\Psi_1$  and  $\Psi_2$  must coincide. The second term imposes actuation slip of intensity  $\bar{f}$  that is tangent to a deformed isoline  $\nabla\bar{\Psi}_1$ .

The above formulation is expressed in the same spirit as it is done for conventional contact formulations, see e.g. [3], which is particularly suitable for the finite element method implementation. The necessary FE procedures have been implemented and derived using the symbolic system *AceGen*, and the subsequent FE analyses were performed in the *AceFEM* environment [4].

### Exemplary 2D FEM results

The results of an exemplary analysis of a two-dimensional contracting actuator are shown in Fig. 3. The actuator consists of two  $20 \times 10 \text{ mm}^2$  rectangles, clamped at opposite sides, with the initial 5 mm overlap. A plain-strain hyperelastic model for both parts is assumed, with the Young's modulus  $E = 1 \text{ MPa}$  and Poisson's ratio  $\nu = 0.4$ .



Figure 3: Left: initial mesh ( $\bar{f} = 0$ ). Right: deformed mesh ( $\bar{f} = 0.03 \text{ [N/mm}^3\text{]}$ ).

In Fig. 4, the non-uniform deformation with horizontally-aligned stress gradients in the contact zone is presented, which is characteristic of volumetric actuators.

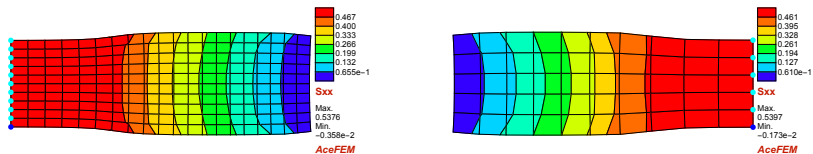


Figure 4:  $S_{xx}$  stress field in the deformed configuration for the left and right part of the actuator ( $\bar{f} = 0.03 \text{ [N/mm}^3\text{]}$ ).

**Acknowledgement** Work supported by the project “Micromechanics of Programmable Matter” (contract no. 2011/03/D/ST8/04089 with the National Science Centre in Poland)

### References

- [1] McNeill Alexander R.: Principles of Animal Locomotion. Princeton, US, 2006.
- [2] Lengiewicz J., Kurasa M., Hołobut P.: Modular-robotic structures for scalable collective actuation. *Robotica*, doi:10.1017/S026357471500082X, 2015.
- [3] Lengiewicz J., Korelc J., Stupkiewicz S.: Automation of finite element formulations for large deformation contact problems. *Int.J.Numer.Meth.Eng.* 85:1252–1279, 2011.
- [4] Korelc J.: *AceGen* and *AceFEM* user manuals. Available at <http://www.fgg.uni-lj.si/Symech/>, 2009.